THREE-DIMENSIONAL ARBITRARY LAGRANGIAN–EULERIAN NUMERICAL PREDICTION METHOD FOR NON-LINEAR FREE SURFACE OSCILLATION

SATORU USHIJIMA*

Central Research Institute of Electric Power Industry, 1646 Abiko Abiko-shi, Chiba-ken, 270-11, Japan

SUMMARY

A numerical prediction method has been proposed to predict non-linear free surface oscillation in an arbitrarily-shaped three-dimensional container. The liquid motions are described with Navier–Stokes equations rather than Laplace equations which are derived by assuming the velocity potential. The profile of a liquid surface is precisely represented with the three-dimensional curvilinear co-ordinates which are regenerated in each computational step on the basis of the arbitrary Lagrangian–Eulerian (ALE) formulation. In the transformed space, the governing equations are discretized on a Lagrangian scheme with sufficient numerical accuracy and the boundary conditions near the liquid surface are implemented in a complete manner. In order to confirm the applicability of the present computational technique, numerical simulations are conducted for the free oscillations of viscid and inviscid liquids and for highly non-linear oscillation. In addition, non-linear sloshing motions caused by horizontal and vertical excitations and a transition from non-linear sloshing to swirling are numerically predicted in three-dimensional cylindrical containers. Conclusively, it is shown that these sloshing motions associated with high non-linearity are reasonably predicted with the present numerical technique. © 1998 John Wiley & Sons, Ltd.

KEY WORDS: arbitrary Lagrangian–Eulerian method; body-fitted co-ordinates; free surface; non-linear sloshing; Navier–Stokes equation

1. INTRODUCTION

The dynamic oscillation of liquid with a free surface has long been of interest in a variety of engineering fields. In particular, non-linear sloshing with large amplitudes and more complicated swirling motions are sometimes considered as the most important phenomena associated with the engineering design and assessment. Since neither theoretical analyses nor linear calculations are available for these problems [1], computational techniques are expected to become one of the most effective methods with which to obtain accurate solutions.

The computational techniques proposed in the past for non-linear sloshing have often employed the velocity potential in the numerical models and the governing equations were usually solved with boundary element methods [2,3] and finite element methods [4]. Although the velocity potential models might be useful in terms of computational efficiency, it is largely

---

* Correspondence to: Central Research Institute of Electric Power Industry, 1646 Abiko Abiko-shi, Chiba-ken, 270-11, Japan. Tel.: + 81 0471 821181; fax: + 81 0471 847142; e-mail: ushijima@criepi.denken.or.jp

uncertain whether the actual three-dimensional flows accompanied by non-linear oscillations and swirling motions of free surfaces can be treated adequately by assuming that the flows are irrotational and that the liquid viscosity is negligible.

On the other hand, fewer attempts have been made to numerically predict the sloshing problems using complete Navier–Stokes equations. While in some cases finite difference methods were employed with the VOF techniques [5] and the MAC methods [6], it is obvious that the numerical schemes based on the Eulerian computational grids have disadvantages in maintaining sufficient numerical accuracy near the largely and unsteadily deformed liquid surfaces. In more advanced numerical techniques, arbitrary Lagrangian–Eulerian (ALE) formulation [7] and Lagrangian grid formulations are adopted to represent the profile of a liquid surface, and Navier–Stokes equations are solved with finite element methods [8,9] and finite difference techniques [10]. However, many are applicable only to two-dimensional problems. Thus, it seems that there have been very few numerical techniques which can deal with three-dimensional liquid behaviors where the free surfaces are deformed unsteadily and non-uniformly, and, at the same time, which can preserve sufficient numerical accuracy in the solution procedure of Navier–Stokes equations on suitable computational grids.

In the present study, a new computational technique is proposed to predict non-linear sloshing problems in an arbitrarily-shaped three-dimensional liquid region. The liquid motions are described with Navier–Stokes equations rather than velocity potential models. The profile of a liquid surface is accurately represented by the three-dimensional curvilinear co-ordinates which are regenerated in each computational step on the basis of the ALE formulation. Since the boundary conditions near the free surface can be implemented completely in the computational space, the present method is particularly advantageous to the usual techniques in which Eulerian computational grids are adopted. Moreover, in this transformed space, the governing equations are discretized on a Lagrangian scheme in which numerical accuracy is preserved at a sufficient level.

In order to confirm the applicability of the present computational technique, numerical simulations are performed for the free oscillations of viscid and inviscid liquids and for highly non-linear oscillations. In addition, the present technique is applied to three-dimensional sloshing problems in cylindrical tanks in various conditions: non-linear sloshing motions when horizontal and vertical excitations are imposed, and a transition from non-linear sloshing to swirling when an initial trigger is provided vertically to the principal excitation. Conclusively, it is shown that the non-linear sloshing and swirling motions are reasonably predicted with the present numerical technique.

2. NUMERICAL PROCEDURE

2.1. Grid generation

The non-orthogonal curvilinear co-ordinates are regenerated in each computational time step in order to adequately represent the shape of the free surface, which is deformed unsteadily and non-uniformly, at every moment. In contrast to the Lagrangian grid generation, the ALE formulation allows us to create curvilinear co-ordinates independently of the liquid motion, which means that the velocity of the computational grid point may not coincide with that of the liquid. Thus, once the shape of the free surface is specified, the corresponding curvilinear co-ordinates are generated in an arbitrarily-shaped three-dimensional liquid region, taking this profile as one of the boundary conditions with the following equations. These

equations are derived from Poisson equations by interchanging dependent and independent variables [11]:

$$\left(\frac{\partial^2 x_i}{\partial \xi_p \partial \xi_q}\right)^* \left(\frac{\partial \xi_p}{\partial x_j}\right)^* \left(\frac{\partial \xi_q}{\partial x_j}\right)^* + \frac{\partial^2 x_i}{\partial \xi_r \partial \xi_s}\left(\frac{\partial \xi_r}{\partial x_j}\right)^* \left(\frac{\partial \xi_s}{\partial x_j}\right)^* + P_m\left(\frac{\partial x_i}{\partial \xi_m}\right)^* = 0, \tag{1}$$

where x_i and ξ_m are the three-dimensional spatial co-ordinates in physical and computational (or transformed) spaces, respectively. In Equation (1), $p \neq q$ and $r = s$, and the Einstein summation rule is applied to the terms in this paper which have the same subscripts. The control functions P_m are utilized to adjust the grid intervals in the physical space [11]. The derivatives with asterisks in Equation (1) are not evaluated using the usual central difference, but from cubic spline interpolations as proposed by Ushijima [12], so that the metric coefficients can preserve a higher accuracy than the usual grid generation method.

A unit computational volume in the transformed space consists of 27 grid points as shown in Figure 1. All of their locations in the physical space are determined by solving Equation (1). The pressure variable is placed at the center grid in the unit volume, while each contravariant velocity component is defined at the center grid on the corresponding surface. In contrast to such staggered arrangements inside the computational domain, the grid distributions are varied near the free surface and rigid boundaries; the physical quantities are defined only on the transformed boundary surfaces so that Dirichlet boundary conditions can be implemented exactly. In addition, when a certain physical value at a grid point needs to be evaluated at a point located in a different position, this value is interpolated with cubic spline functions in the computational domain rather than simple linear interpolation.

2.2. Equation of motion

The incompressible liquid motion with a free surface is described by Navier–Stokes equations rather than velocity potential, so that the three-dimensional flows can be treated more generally as rotational and viscid liquid behaviors. The governing equations are transformed into those in the computational space, which are given by

$$\frac{\mathrm{D}u_i}{\mathrm{D}t} = -\frac{1}{\rho}\frac{\partial p}{\partial \xi_m}\frac{\partial \xi_m}{\partial x_i} + F_i + \nu\left(\frac{\partial^2 u_i}{\partial \xi_m \partial \xi_n}\frac{\partial \xi_m}{\partial x_j}\frac{\partial \xi_n}{\partial x_j} + P_m\frac{\partial u_i}{\partial \xi_m}\right). \tag{2}$$

Here u_i, p, ρ and ν are velocity component in x_i direction, pressure, liquid density and kinematic viscosity, respectively. The gravity and the forced acceleration imposed to cause a sloshing motion is represented by F_i in Equation (2). Since the ALE formulation is employed, the Lagrangian differential operator in Equation (2) is given by the following form [13]:

$$\frac{\mathrm{D}}{\mathrm{D}t} = \frac{\partial}{\partial \tau} + (U_m - U_{0m})\frac{\partial}{\partial \xi_m}, \tag{3}$$

where t and τ are time in physical and computational spaces respectively, and are set to be identical in the present computation. The contravariant velocity components U_m and U_{0m} represent the velocity of the liquid and that of the computational grid point respectively, and are defined by

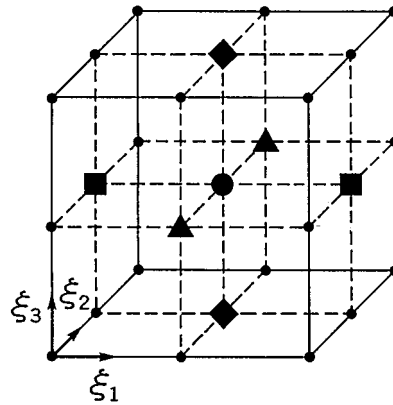$$U_m = u_i\frac{\partial \xi_m}{\partial x_i}, \tag{4a}$$

and

Figure 1. A unit computational volume in the transformed space ($\bullet$, scalar value; $\blacksquare$, U_1; $\blacktriangle$, U_2; $\blacklozenge$, U_3).

$$U_{0m} = \frac{\partial x_i}{\partial \tau} \frac{\partial \xi_m}{\partial x_i}. \tag{4b}$$

The transformed momentum equations are discretized on a Lagrangian scheme in the computational space. For convenience, Equation (2) may be expressed in the following form:

$$\frac{Du_i}{Dt} = -PG_i + F_i + D_i \equiv FU_i, \tag{5}$$

where PG_i and D_i stand for the pressure gradient and diffusion terms in Equation (2) respectively. Taking account of the Taylor expansion for total differentiation up to the second-order terms, Equation (5) can be discretized in the following form as proposed by Ushijima [12]:

$$u_i^{n+1} = u_i'^n + \left(\frac{3}{2} FU_i'^n - \frac{1}{2} FU_i''^{n-1} \right)\Delta t + \Delta^3. \tag{6}$$

Here the superscript n means the computational time step number, where $t = n\Delta t + t_0$, and prime and double prime stand for the spatial location at the upstream points $P'(\xi_1', \xi_2', \xi_3')$ and $P''(\xi_1'', \xi_2'', \xi_3'')$ respectively. The positions of P' and P'' in the computational space are given by

$$\xi_m' = \xi_m - (U_m^n - U_{0m}^n)\Delta t \tag{7a}$$

$$\xi_m'' = \xi_m - (U_m^n - U_{0m}^n)\Delta t - (U_m'^{n-1} - U_{0m}'^{n-1})\Delta t. \tag{7b}$$

The pressure-gradient term included on the right hand side of Equation (6) is dealt with implicitly:

$$PG_i^{n+1} = \frac{3}{2} PG_i'^n - \frac{1}{2} PG_i''^{n-1}. \tag{8}$$

The acceleration term is treated in the first-order accuracy with respect to time. Thus, Equation (6) finally becomes

$$u_i^{n+1} = u_i'^n + \left[-PG_i^{n+1} + F_i^n + \left(\frac{3}{2} D'^n - \frac{1}{2} D_i''^{n-1} \right) \right]\Delta t. \tag{9}$$
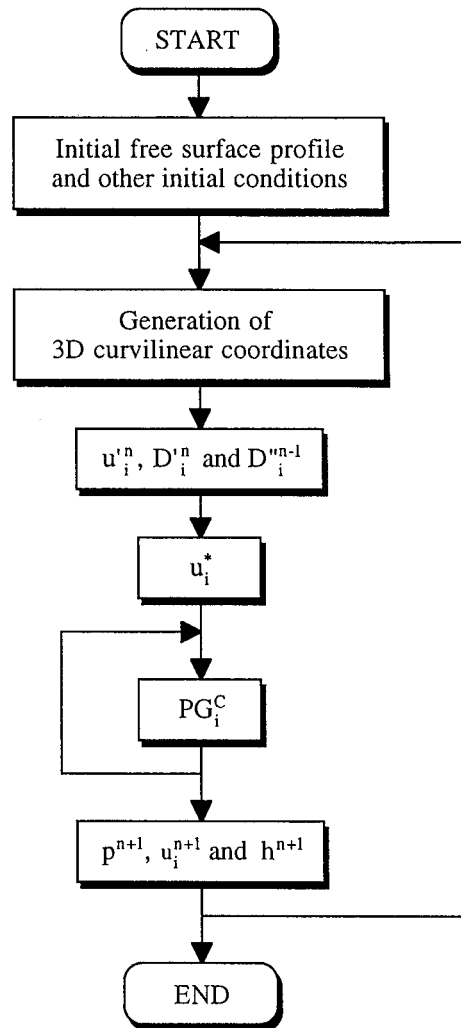
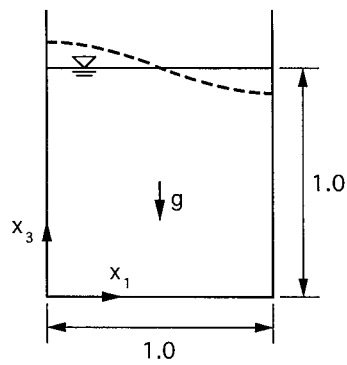Figure 2. Flowchart for solution procedures.
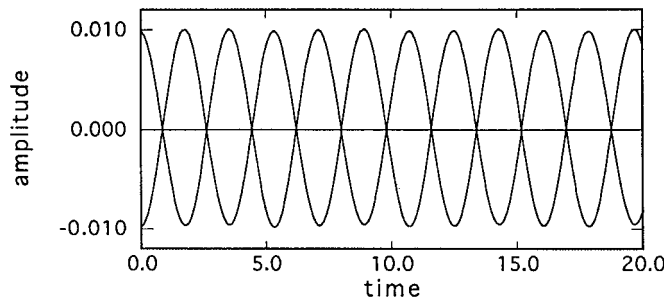

Figure 3. A two-dimensional container.

Figure 4. Time history of free surface displacement without viscous effect.

The first term on the right hand side of Equation (9), corresponding to the convection term, is calculated with the spatial interpolation in which local cubic spline interpolation is utilized in the three-dimensional computational space [12]. The following cubic spline function $S_m(\xi_m)$ is derived in the ξ_m direction to interpolate the physical value ϕ, located between $\xi_{m_{i-1}}$ and ξ_{m_i}, using second-order derivatives M_{i-1}, and M_i:

$$S_m(\xi_m) = M_{i-1} \frac{(\xi_{m_i} - \xi_m)^3}{6h_i} + M_i \frac{(\xi_m - \xi_{m_{i-1}})^3}{6h_i}$$

$$+ \left(\phi_{i-1} - \frac{M_{i-1}h_i^2}{6}\right)\frac{\xi_{m_i} - \xi_m}{h_i} + \left(\phi_i - \frac{M_i h_i^2}{6}\right)\frac{\xi_m - \xi_{m_{i-1}}}{h_i}, \tag{10}$$

where $h_i = \xi_{m_i} - \xi_{m_{i-1}}$. The second-order derivatives are evaluated with a third-order polynomial, which is uniquely determined from the four neighboring physical values located at $\xi_{m_{i-2}}$ to $\xi_{m_{i+1}}$. The similar spatial interpolation is performed in all directions, as a result of which the convection term is evaluated with third-order accuracy.

2.3. Pressure calculation and velocity correction

The calculation of pressure and velocity correction substantially follow the SMAC method [14]. At first, the tentative pressure gradient term PG_i^* is calculated by assuming the pressure field to be given by the hydrostatic pressure distribution. Thus the corresponding velocity u_i^* is calculated from
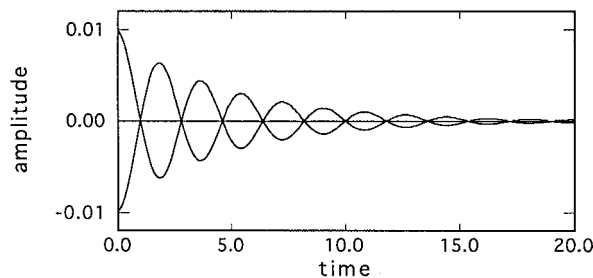

Figure 5. Time history of free surface displacement with viscous effect.

$$u_i^* = u_i'^n + \left[-PG_i^* + F_i^n + \left(\frac{3}{2} D_i'^n - \frac{1}{2} D_i''^{n-1} \right) \right] \Delta t. \tag{11}$$

With Equations (9) and (11), the following relationship is derived:

$$u_i^C = -PG_i^C \Delta t, \tag{12}$$

where

$$u_i^C = u_i^{n+1} - u_i^*, \tag{13}$$

and

$$PG_i^C = PG_i^{n+1} - PG_i^*. \tag{14}$$

Setting the liquid continuity to be satisfied at the $n+1$ computational step as suggested by Harlow and Welch [15], the following equation is obtained:

$$\frac{\partial u_i^{n+1}}{\partial x_i} = \frac{\partial u_i^C}{\partial x_i} + \frac{\partial u_i^*}{\partial x_i} = 0. \tag{15}$$

Accordingly, the correction term PG_i^C can be derived from the tentative velocity u_i^* with the following relationship:

$$\frac{\partial PG_i^C}{\partial x_i} \Delta t = \frac{\partial u_i^*}{\partial x_i}. \tag{16}$$

Once the correction term PG_i^C is obtained from Equation (16) with iterative calculations, the correction velocity u_i^C can be derived from Equation (12) and finally the velocity u_i^{n+1} at a new computational step is derived from Equation (13). The detailed form of Equation (16) is given by

$$\frac{1}{\rho} \left(\frac{\partial^2 p^C}{\partial \xi_m \partial \xi_n} \frac{\partial \xi_m}{\partial x_i} \frac{\partial \xi_n}{\partial x_j} + P_m \frac{\partial p^C}{\partial \xi_m} \right) \Delta t = \frac{\partial U_m^*}{\partial \xi_m}, \tag{17}$$

where p^C is the correction pressure and U_m^* is the contravariant velocity component defined by

$$U_m^* = u_i^* \frac{\partial \xi_m}{\partial x_i}. \tag{18}$$

2.4. Boundary conditions on free surface

The kinematic free surface condition is determined from the fact that the surface moves with the liquid in the physical space as

$$\frac{\partial h}{\partial t} + u_{Si} \frac{\partial h}{\partial x_i} = u_{S3}, \quad i = 1, 2, \tag{19}$$

where h is the free surface height measured from a standard position and subscript S means that the corresponding values are defined at the grid point on the free surface. In particular, x_3 is a vertically upward co-ordinate in the Cartesian system and u_{S3} is the velocity component in physical space toward x_3 direction. The Equation (19) is transformed into the following form:

$$\frac{\partial h}{\partial t} + (U_{Sm} - U_{0Sm}) \frac{\partial h}{\partial \xi_m} = u_{S3}, \quad m = 1, 2, \tag{20}$$

where U_{0Sm} is the contravariant velocity on the liquid surface. The kinematic condition given in Equation (20) can be discretized on the Lagrangian scheme in a similar way to the discretization of momentum equations.

When the viscous stresses on a liquid–gas interface are negligible, the stress conditions on free surfaces are determined by the following two equations:

$$n_i \sigma_{ij} n_j = Sk, \tag{21}$$

$$\tau_i \sigma_{ij} n_j = 0, \tag{22}$$

where S and k mean the coefficient of surface tension and the curvature of the free surface, respectively. The unit vectors n_i and τ_i are normal and tangential to the free surface and the stress tensor σ_{ij} is defined by

$$\sigma_{ij} = -p_0 \delta_{ij} + \mu \left(\frac{\partial u_i}{\partial x_j} + \frac{\partial u_j}{\partial x_i} \right), \tag{23}$$

where p_0 is the atmospheric pressure and μ is the dynamic viscosity. From the above conditions, the following results can be derived in the computational space

$$\frac{\partial u_i}{\partial \xi_3} \equiv \left(FS_i - \frac{\partial u_i}{\partial \xi_1} \frac{\partial \xi_1}{\partial x_3} - \frac{\partial u_i}{\partial \xi_2} \frac{\partial \xi_2}{\partial x_3} \right) \left(\frac{\partial \xi_3}{\partial x_3} \right)^{-1} \quad i = 1, 2, 3, \tag{24}$$

with

$$FS_1 = -\frac{\partial u_3}{\partial \xi_m} \frac{\partial \xi_m}{\partial x_1} + 2\frac{\partial h}{\partial \xi_m} \frac{\partial \xi_m}{\partial x_1} \frac{\partial u_1}{\partial \xi_n} \frac{\partial \xi_n}{\partial x_1} - \frac{\partial h}{\partial \xi_m} \frac{\partial \xi_m}{\partial x_1} \left(\frac{Sk + p_0}{\mu} \right) + \frac{\partial h}{\partial \xi_m} \frac{\partial \xi_m}{\partial x_2} \left(\frac{\partial u_1}{\partial \xi_n} \frac{\partial \xi_n}{\partial x_2} + \frac{\partial u_2}{\partial \xi_n} \frac{\partial \xi_n}{\partial x_1} \right) \tag{25a}$$

$$FS_2 = -\frac{\partial u_3}{\partial \xi_m} \frac{\partial \xi_m}{\partial x_2} + 2\frac{\partial h}{\partial \xi_m} \frac{\partial \xi_m}{\partial x_2} \frac{\partial u_2}{\partial \xi_n} \frac{\partial \xi_n}{\partial x_2} - \frac{\partial h}{\partial \xi_m} \frac{\partial \xi_m}{\partial x_2} \left(\frac{Sk + p_0}{\mu} \right) + \frac{\partial h}{\partial \xi_m} \frac{\partial \xi_m}{\partial x_1} \left(\frac{\partial u_2}{\partial \xi_n} \frac{\partial \xi_n}{\partial x_1} + \frac{\partial u_1}{\partial \xi_n} \frac{\partial \xi_n}{\partial x_2} \right) \tag{25b}$$

$$FS_3 = \left(\frac{\partial h}{\partial \xi_l} \frac{\partial \xi_l}{\partial x_a} \right) \left(\frac{\partial h}{\partial \xi_m} \frac{\partial \xi_m}{\partial x_b} \right) \frac{\partial u_a}{\partial \xi_n} \frac{\partial \xi_n}{\partial x_b} - \left[\left(\frac{\partial h}{\partial \xi_m} \frac{\partial \xi_m}{\partial x_1} \right)^2 + \left(\frac{\partial h}{\partial \xi_n} \frac{\partial \xi_n}{\partial x_2} \right)^2 - 1 \right] \frac{Sk + p_0}{2\mu} \quad a, b = 1, 2. \tag{25c}$$

In a case, which will be described later, where the present numerical method is applied to the examples of sloshing problems, it is assumed that the atmospheric pressure equals zero and that the effect of surface tension can be neglected.

2.5. Solution procedure

The main solution procedures in the present numerical method can be summarized as shown in Figure 2. First of all, initial free surface profile and other necessary initial conditions are specified. Then the three-dimensional curvilinear co-ordinates, which are coincident with the provided free surface and the other fixed boundary shapes, are generated. In the computational space corresponding to the generated co-ordinates, the numerical procedure for liquid calculations is performed. The convection and diffusion terms are first evaluated on a Lagrangian scheme, and approximate velocity u_i^* is derived using these values. The converged correction pressure is obtained in the iterative calculations and velocity components and free surface levels are finally derived at a new computational step. When the unsteady numerical prediction still proceeds, the free surface profile is updated and new curvilinear co-ordinates are generated. In this way, unsteady numerical procedure continues until the appointed time.
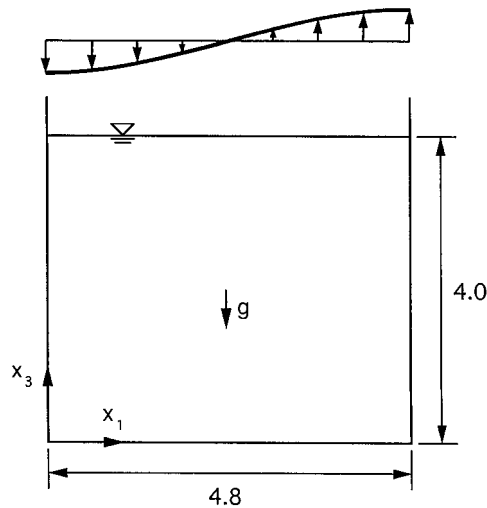
Figure 6. Dimensions of a two-dimensional container.

3. FREE SURFACE OSCILLATION IN TWO-DIMENSIONAL CONTAINER

3.1. Free oscillation

The numerical analysis of the free oscillation of a liquid with a small amplitude allows us to confirm that the numerical technique satisfies the necessary specifications, such as mass and momentum conservation. The present example follows the same condition adopted by Ramaswamy [9]; the two dimensional rectangular container, as shown in Figure 3 is 1.0 units in width and 1.0 units in height, and the gravity acts downward with a unit magnitude. The initial profile of the free surface is given by

$$h = 1.0 + a \sin[\pi(0.5 - x_1)] \tag{26}$$

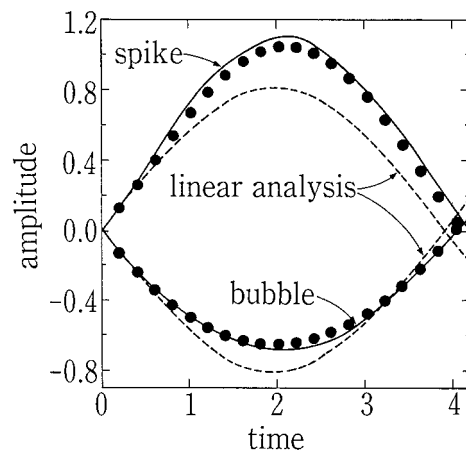where the amplitude of the antisymmetric natural mode equals 0.01 units.

Figure 7. Time history of free surface displacement (●, present results; —, Harlow and Welch [16]).
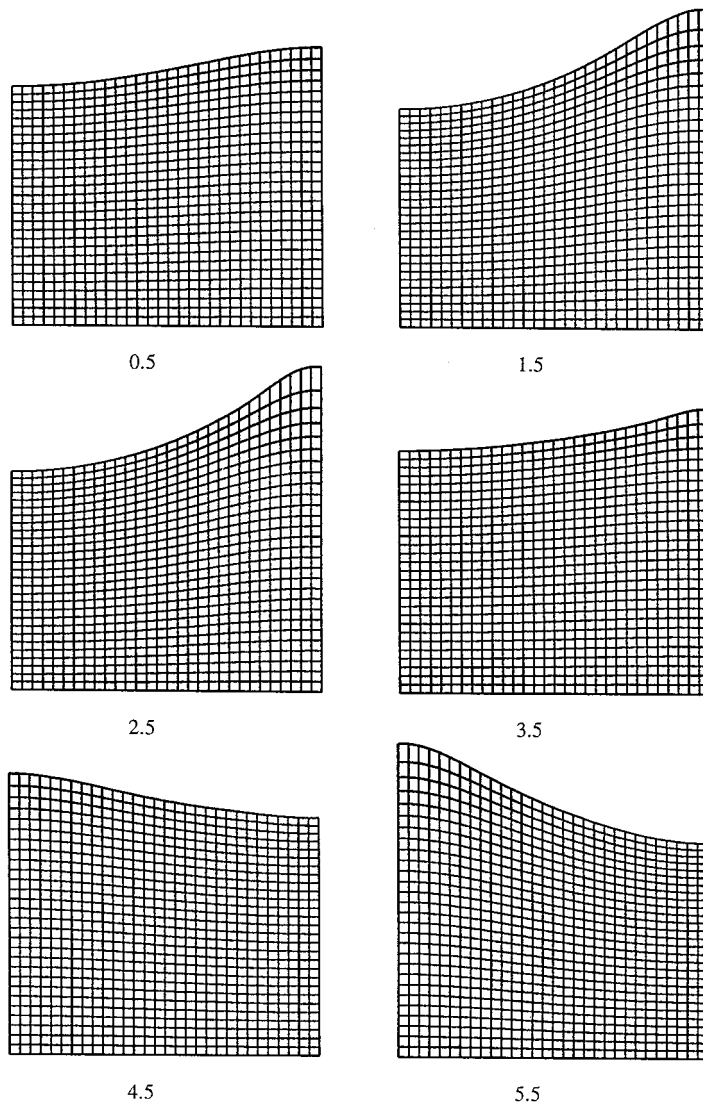
Figure 8. Generated curvilinear co-ordinates by ALE method.

Figure 4 shows the time history of the free surface displacements at both ends, $x_1 = 0$ and 1.0, calculated with the non-viscosity condition, in which the free-slip condition is given on all solid boundaries of the container, and liquid viscosity is set at zero. As shown in this figure, no numerical damping effects are found and the conservation of mass and momentum is completely satisfied. On the other hand, Figure 5 shows the time history of the amplitude calculated with the viscous condition, in which liquid velocity on the solid boundaries is zero and kinematic viscosity of the liquid equals 0.01 units. The adequate attenuation of the wave amplitudes is observed in the result, which has a similar tendency to the numerical results presented by Ramaswamy [9].

3.2. Non-linear oscillation

The present example was chosen in multiple previous numerical studies as done by Harlow and Welch [16], Ramaswamy [9], Takizawa [10] and others, in order to demonstrate the validity of the computing technique for highly non-linear oscillation. As shown in Figure 6, the rectangular container is 4.8 units in width and 4.0 units in height. A gravity acceleration of one unit acts downwards and the cosine pressure impulse is imposed on the free surface of the liquid in the container. The pressure pulse is defined by

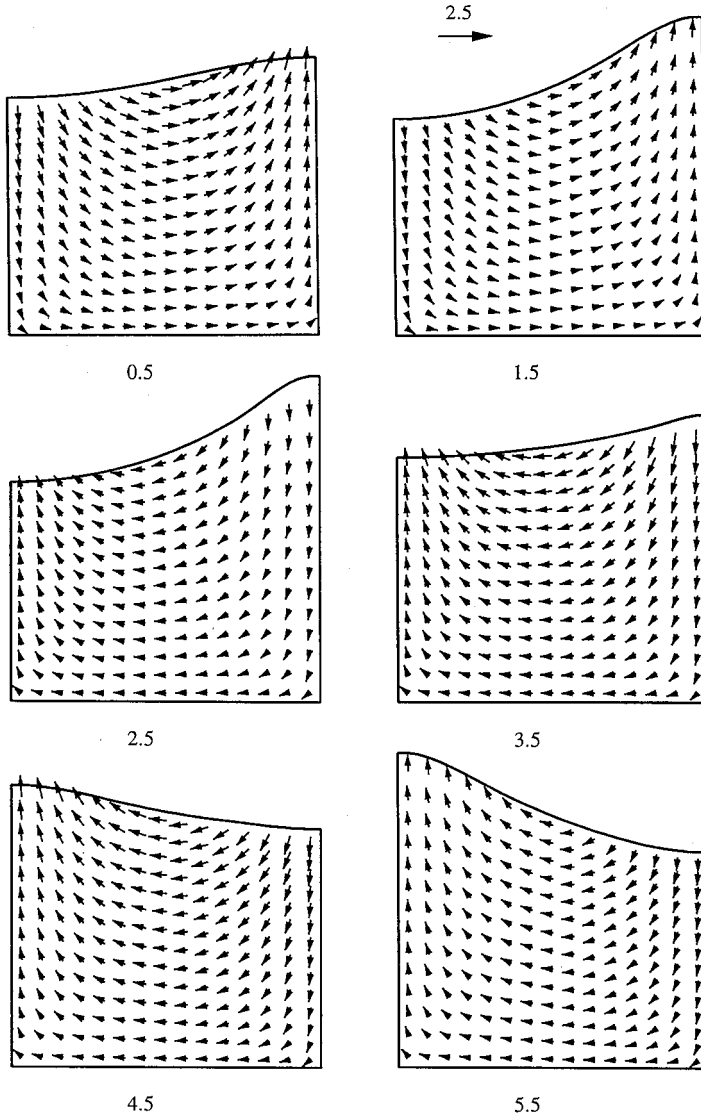$$p_0(t) = A \, \delta(T) \cos(kx_1), \tag{27}$$
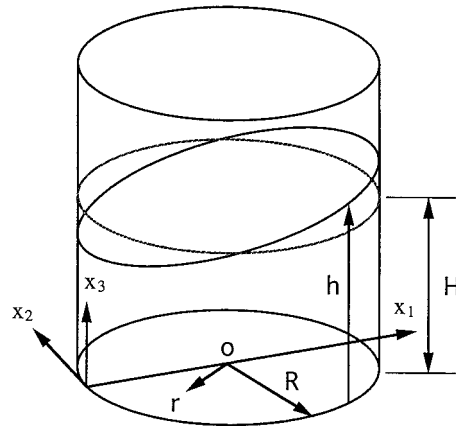

Figure 9. Calculated velocity vectors.

Figure 10. Definition sketch of a three-dimensional cylindrical tank.

where $\delta(t)$ is the dirac delta function and the amplitude A equals 1.0 units. The disturbance wave number k is given by $2\pi/9.6$. The liquid kinematic viscosity is defined by $v = 0.01$ units and the free-slip condition is imposed on the solid boundaries of the container.

The time history of the free surface displacements is shown in Figure 7, in which the amplitudes of the linear analysis and the numerical results calculated by Harlow and Welch [16] are also presented. The present results in Figure 7 show the highly non-linear spike and bubble, which are quite similar to the results of Harlow and Welch [16]. The generated computational grid distributions are shown in Figure 8 and the predicted velocity vectors are presented in Figure 9. It can be seen that the adequate mesh regeneration is maintained and that the reasonable liquid motions are predicted in the calculation.

4. THREE-DIMENSIONAL SLOSHING IN CYLINDRICAL TANK

4.1. Forced horizontal oscillation

Figure 10 illustrates the definition sketch, in which Cartesian co-ordinates and dimensions are indicated, where R and H, correspond to the radius of a cylindrical tank, and liquid depth in a static condition. In a cylindrical tank with $R = H = 0.5$ m, the liquid with the kinematic viscosity of 0.01 cm^2 s^{-1} is subject to the forced acceleration in x_1, with the direction given by
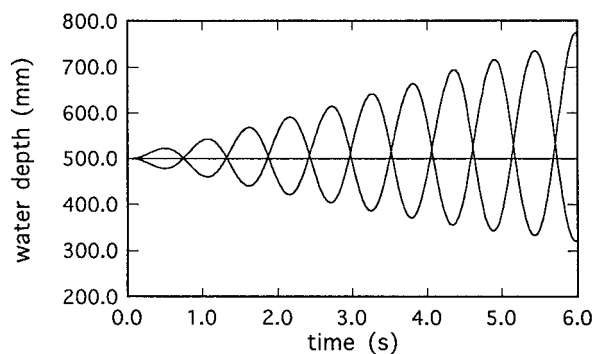

Figure 11. Time history of free surface displacement in (1, 1) mode non-linear sloshing.
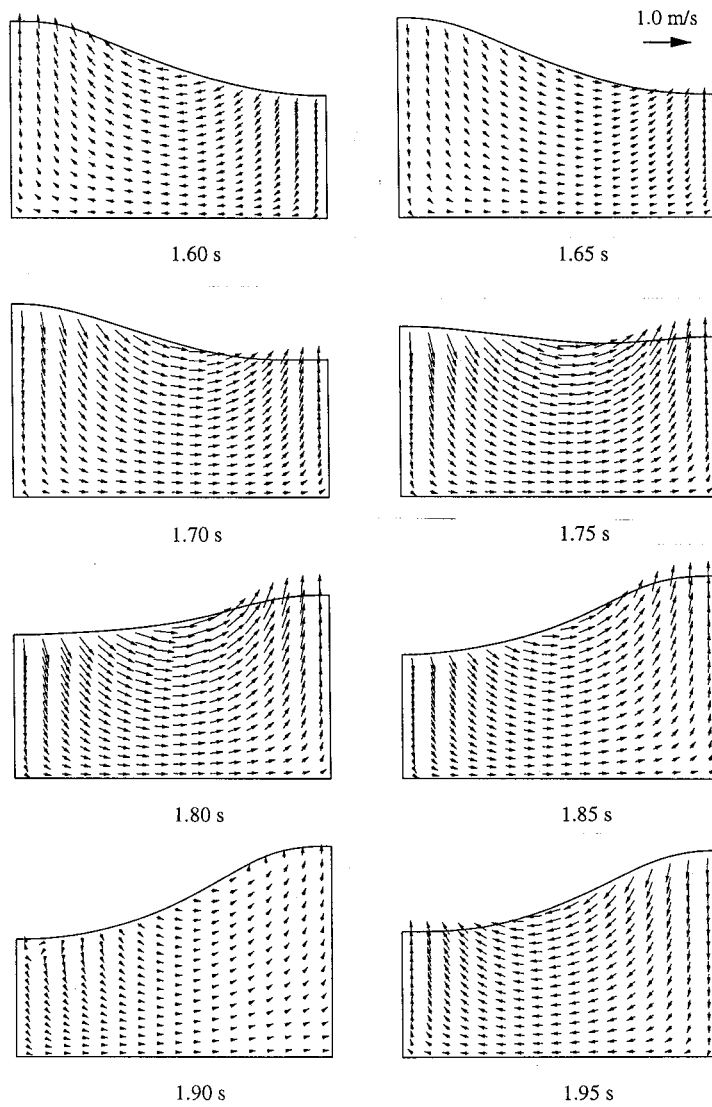
Figure 12. Computed velocity vectors in (1, 1) mode non-linear sloshing.

$$a_1(t) = -X_1\omega^2 \sin(\omega t), \tag{28}$$

where the amplitude X_1, and angular frequency ω of the forced displacement in the x_1 direction are 10 mm and 5.85 radian s^{-1}, respectively. This external vibration coincides with the (1, 1) mode of the natural frequency [17]. Figure 11 shows the time history of the free surface displacements at $(x_1, x_2) = (0, 0)$ and $(2R, 0)$. The upward amplitude of the sloshing becomes larger than the downward amplitude as time increases, indicating the typical non-linear characteristic of the free surface sloshing. The present results are quite similar to those reported by Kasuga *et al.* [18], although the present amplitudes are slightly larger than their results which were obtained with the assumption of velocity potential. Figure 12 shows the velocity vectors and free surface profile on the x_1–x_3 vertical section.

In addition, Figure 13 shows the three-dimensional view of the generated curvilinear co-ordinates in the computation for the $(1, 2)$ mode of the natural frequency. In this calculation, X_1 and ω, in Equation (28) are set at 2 mm and 10.22 radian s^{-1}, respectively.

4.2. Forced vertical oscillation

The liquid sloshing in a cylindrical tank which is subject to the vertical oscillation is numerically predicted by the present computational method. The dimensions of the cylindrical tank are $R = 100$ mm and $H = 200$ mm. The initial profile of the free surface is assumed to be given by

$$h = H + 0.02R \cos\left(\frac{\pi r}{R}\right), \tag{29}$$

and initial velocity in all directions is set at zero. The liquid in the tank is subject to the following vertical acceleration:

$$a_3(t) = -X_3\omega^2 \cos(\omega t), \tag{30}$$

where X_3 and $\omega/2\pi$ are the amplitude and frequency of the vertical oscillation, and are given by 2.0 mm and 6.168 s^{-1}, respectively.

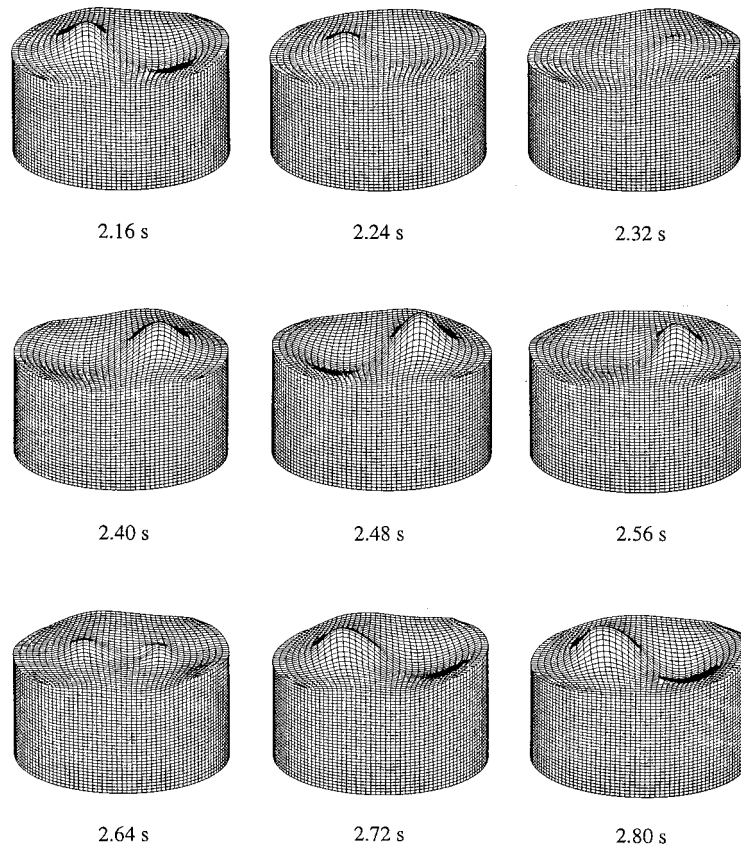|		
2.16 s	2.24 s	2.32 s
2.40 s	2.48 s	2.56 s
2.64 s	2.72 s	2.80 s

Figure 13. Perspective views of free surface oscillation in $(1, 2)$ mode non-linear sloshing.
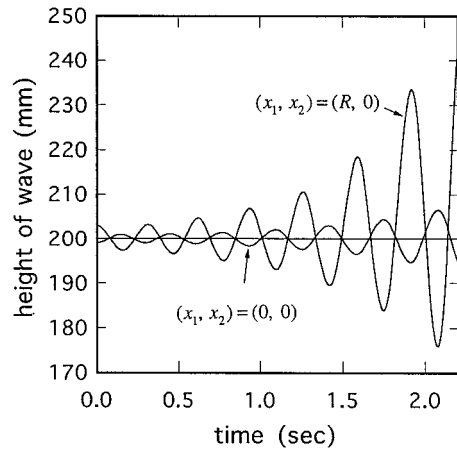
Figure 14. Time history of free surface displacement in vertical oscillation.

Figure 14 shows the time history of the amplitudes at $(x_1, x_2) = (0, 0)$ and at the center of the tank, $(R, 0)$. As shown in Figure 14, the development of the (0, 1) mode 1/2-subharmonic response is satisfactorily calculated, in which highly non-linear oscillation can be seen. The profile of the free surface is compared between calculated results and experimentally observed data [19] in Figure 15. While the computed free surface profile develops unsteadily, the results at $t = 1.1$ s and $t = 1.92$ s agree reasonably with the experimental ones. Figure 16 shows the velocity vectors and deformed free surface on the x_1-x_3 vertical section during the non-linear sloshing.

4.3. Swirling motion of free surface

It has been reported that when an axisymmetrical tank of liquid is subject to a harmonic vibration in a single horizontal direction, the free surface motion may rotate harmonically or non-harmonically around the vertical axis of the tank. This swirling motion of waves was
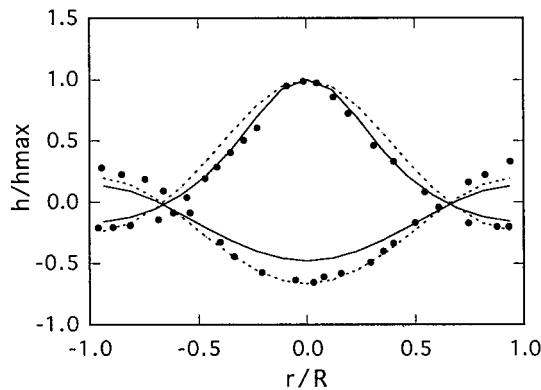

Figure 15. Free surface profiles in vertical oscillation (●, Dodge *et al.* [19]; - - - -, $t = 1.10$ s and 1.26 s; —, $t = 1.75$ s and 1.92 s).
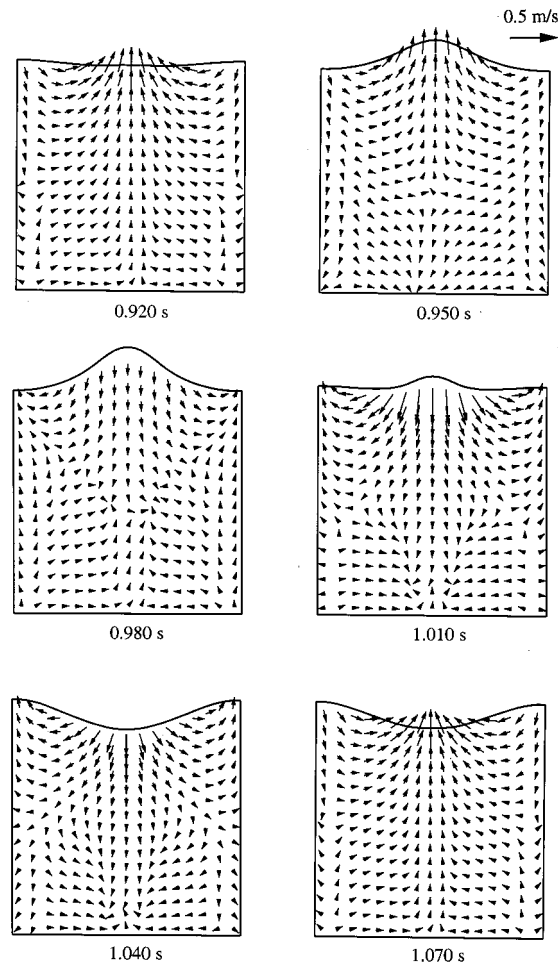
Figure 16. Computed velocity vectors and free surface profiles in vertical oscillation.

observed by Hutton [20] in a cylindrical tank laterally oscillated at frequencies just below the lowest natural frequency. Several experimental and theoretical investigations regarding this type of wave motion have been attempted [21]. However, only a few numerical predictions associated with this phenomenon have been reported [22,23]. Tanaka and Nakayama [22] have numerically simulated a swirl motion by a boundary element method with the assumption of irrotational flow of an inviscid liquid. Arai *et al.* [23] attempted to compute swirling waves based on a MAC method by setting the initial free surface gradient in the direction vertical to the forced vibration. In the present investigation, a transition from non-linear sloshing to swirling motions in a cylindrical tank is numerically predicted by setting up the same initial trigger in the x_2-direction, as employed by Tanaka and Nakayama

$$a_2(t) = \begin{cases} X_2 \sin(2\pi f t), & 0 \leq t \leq 3 \text{ (s)} \\ 0, & 3(\text{s}) < t \end{cases} \tag{31}$$

while the following harmonic vibration is continuously imposed in x_1-direction:

$$a_1(t) = X_1 \sin(2\pi f t), \quad 0 \leq t, \tag{32}$$

where $X_1 = -0.0178$ g and $X_2 = X_1 \sin(\pi t/6)$. The geometries of the cylindrical tank are $R = 0.5$ m and $H = 0.6$ m. The liquid in the tank is assumed to have no viscosity and free-slip boundary conditions are utilized on the solid boundaries. While the natural frequency of the (1, 1) mode equals 0.944 Hz in the present geometries, the calculation is performed by setting $f = 0.940$, as done by Tanaka and Nakayama.

Figures 17(a) and (b) show the surface displacements at $(x_1, x_2) = (0, 0)$ and $(2R, 0)$, and $(x_1, x_2) = (R, -R)$ and (R, R), respectively. On the plane of principal excitation, as shown in Figure 17(a), a large non-linear response develops gradually. On the other hand, while relatively small oscillation continues on x_2–x_3 plane in the initial stage, as shown in Figure 17(b), the amplitudes becomes larger at about $t = 10$ s, which indicates the transition to swirling motion of the free surface. Although the present results are slightly different from those predicted by Tanaka and Nakayama, possibly because their computational method was based on a velocity potential model, the transition from large planar motion to swirling motions is numerically predicted in quite a similar way to their results.

5. CONCLUDING REMARKS

A new computational technique has been proposed to numerically predict non-linear sloshing problems in an arbitrarily-shaped three-dimensional liquid region. In the present method, the liquid motions are described with complete Navier–Stokes equations rather than velocity potential models, which have mainly been employed in the usual numerical method for sloshing. The profile of a free surface is precisely represented with the three-dimensional curvilinear co-ordinates which are generated in each computational step on the basis of the ALE formulation. Since the boundary conditions near the free surface can be completely implemented in the computational space, the present method is particularly advantageous to techniques such as MAC and VOF, in which the Eulerian computational grid is adopted. Moreover, in this transformed space corresponding to the newly generated co-ordinates, the governing equations are discretized on a Lagrangian scheme in which numerical accuracy is preserved satisfactorily.

In order to confirm the applicability of the present computational technique, numerical simulations have been conducted for the free oscillations of viscid and inviscid liquids and for highly non-linear oscillation. As a result, it has been proved that adequate solutions can be obtained for all problems. In addition, three-dimensional sloshing problems in cylindrical tanks have been numerically predicted in various conditions: non-linear sloshing motions when horizontal and vertical excitations are imposed, and a transition from non-linear sloshing to swirling by setting up an initial trigger vertical to the principal excitation. Conclusively, it can be seen that these sloshing motions associated with high non-linearity are reasonably predicted with the present numerical technique.
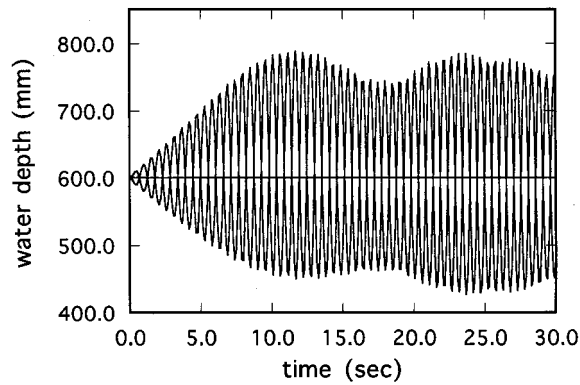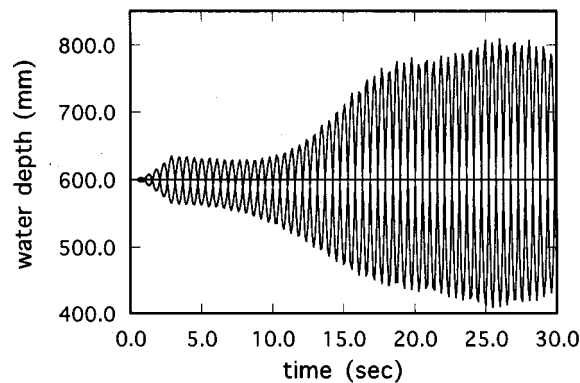
(a) $(x_1, x_2) = (0, 0)$ and $(2R, 0)$

(b) $(x_1, x_2) = (R, -R)$ and (R, R)

Figure 17. Time history of free surface displacement in swirling motion.

REFERENCES

1. H.N. Abramson, 'The dynamic behaviour of liquids in moving containers', *NASA, SP-106* (1966).
2. T. Nakayama and K. Washizu, 'The boundary element method applied to the analysis of two-dimensional nonlinear sloshing problems', *Int. j. numer. methods fluids*, **17**, 1631–1646 (1981).
3. K. Amano, R. Iwano and Y. Shibata, 'Three-dimensional analysis method for sloshing behavior and its application to FBRs', *Nucl. Eng. Des.*, **140**, 297–308 (1993).
4. T. Nakayama and K. Washizu, 'Nonlinear analysis of liquid motion in a container subjected to forced pitching oscillation', *Int. j. numer. methods fluids*, **15**, 1207–1220 (1980).
5. I.S. Partom, 'Application of the VOF method to the sloshing of a fluid in a partially filled cylindrical container', *Int. j. numer. methods fluids*, **7**, 535–550 (1987).
6. M. Nagahama, S. Nagahama, Y. Nekado, T. Yamamori and T. Hori, 'A 3-dimensional analysis of sloshing by means of tank wall fitted coordinate system', *J. Soc. Naval Architects Jap.*, **172**, 487–499 (1992) (in Japanese).
7. C.W. Hirt, A.A. Amsden and J.L. Cook, 'An arbitrary Lagrangian–Eulerian computing method for all flow speeds', *J. Comput. Phys.*, **14**, 227–253 (1974).
8. T. Okamoto, 'Two-dimensional sloshing analysis by Lagrangian finite element method', *Int. j. numer. methods fluids*, **11**, 453–477 (1990).
9. B. Ramaswamy, 'Numerical simulation of unsteady viscous free surface flow', *J. Comput. Phys.*, **90**, 396–430 (1990).

10. A. Takizawa, S. Koshizuka and S. Kondo, 'Generalization of physical component boundary fitted co-ordinate (PCBFC) method for the analysis of free-surface flow', *Int. j. numer. methods fluids*, **15**, 1213–1237 (1992).
11. J.F. Thompson, Z.U.A. Warsi and C.W. Mastin, *Numerical Grid Generation*, Elsevier, New York, 1985.
12. S. Ushijima, 'Prediction of thermal stratification in a curved duct with 3D body-fitted coordinates', *Int. j. numer. methods fluids*, **19**, 647–665 (1994).
13. S. Ushijima, 'Arbitrary Lagrangian–Eulerian numerical prediction for local scour caused by turbulent flows', *J. Comput. Phys.*, **125**, (1996).
14. A.A. Amsden, 'A simplified MAC technique for incompressible fluid flow calculations', *J. Comp. Phys.*, **6**, 322–325 (1970).
15. F.H. Harlow and J.E. Welch, 'Numerical calculation of time-dependent viscous incompressible flow of fluid with free surface', *Phys. Fluids*, **8**, 2182–2189 (1965).
16. F.H. Harlow and J.E. Welch, 'Numerical study of large-amplitude free-surface motions', *Phys. Fluids*, **9**, (1966).
17. H. Lamb, *Hydrodynamics*, 6th Edn., Cambridge University Press, Cambridge, UK, 1932.
18. I. Kasuga, R. Sugino and N. Tosaka, 'Sloshing motion in a cylindrical container by boundary element method', M. Du Q. and T. Honma (eds.), *Boundary Element Methods*, Elsevier, New York, 1993, pp. 315–324.
19. T. Dodge, D.D. Kana and H.N. Abramson, 'Liquid surface oscillations in longitudinally excited rigid cylindrical containers', *AIAA J.*, **3**, 685–695 (1965).
20. R.E. Hutton, 'An investigation of resonant, nonlinear, nonplanar free surface oscillations of a fluid', *NASA Technical Note*, *D-1870* (1963).
21. J.W. Miles, 'Nonlinear surface waves in closed basins', *J. Fluid Mech.*, **75**, 419–448 (1976).
22. H. Tanaka and T. Nakayama, 'A boundary element method for the analysis of nonlinear sloshing in three-dimensional containers', *Trans. JSME*, **57**, 1934–1940 (1991) (in Japanese).
23. M. Arai, L.Y. Chen and Y. Inoue, 'Numerical simulation of sloshing and swirling in a cubic and a cylindrical tank', *J. Kansai Soc. N. A.*, *Jap.*, **219** (1993) (in Japanese).